Tellus (1987), *39A*, 116–137

On the multiplicity of equilibria of baroclinic waves

By MING CAI and MANKIN MAK, *Department of Atmospheric Sciences, University of Illinois, 1101 West Springfield Avenue, Urbana, IL 61801, USA*

(Manuscript received April 1; in final form September 9, 1986)

ABSTRACT

It is shown that, including the null solution (the Hadley state), there can be six different equilibria in a quasi-geostrophic forced dissipative β-plane channel model of a triadic baroclinic wave system. The dependence of the structural, energetics, and stability properties of each equilibrium solution upon the forcing and dissipation parameters have been delineated. Furthermore, the fairly subtle relations among these equilibria have been uniquely identified on the basis of the local bifurcation theory.

Analytic solutions for the viscous single-wave equilibria are obtained. They are unique in contrast to those under an inviscid condition. The latter additionally depend upon the initial state. The diagnosis of the physical character of the single-wave equilibria reveals that such a wave is dynamically neutral with respect to the modified zonal flow. It has identical structural properties as those of a neutral wave according to the linear instability theory.

Two distinctly different classes of multiple-wave equilibria are found numerically. One class is essentially a modified form of the single-wave equilibria. The other class uniquely stems from the presence of wave-wave interaction. A stable single-wave equilibrium and a stable multiple-wave equilibrium are found to coexist in a small part of the parameter domain. The instability of the multiple wave equilibria would result in triad-limit-cycles in this model as previously reported by Mak.

1. Introduction

It was shown in a recent study (Mak, 1985, hereafter referred to as M85) that the equilibrium solution* in a forced dissipative quasigeostrophic triadic baroclinic wave system can consist of either a single wave or multiple waves. They were referred to as the S_{mn} and the M states in that paper. They were found to exist in certain parts of the parameter plane defined by the baroclinic forcing and the dissipation parameters (see Fig. 9 in M85). A number of related fundamental questions were left unanswered. A sample of those questions are: "Do such equilibria only exist in those parameter regions within the range under consideration? Are there additional equilibria? How many equilibria are there at each parameter point? What are the relations among all the equilibria? How are the equilibria related to the triad-limit-cycle? Above all, what is the physical nature of each type of equilibria in the sense of why its structure is as it is?" Answers to these questions would give us considerable insight about the origin and nature of the finite amplitude Rossby waves that might arise from baroclinic instability alone. The purpose of this study is to address those issues in the context of the model used in M85.

The role of topography is deliberately not considered in this study. The dynamics of equilibria in a geophysical model with topography has been the subject of many investigations in recent years (e.g., Charney and DeVore, 1979; Pedlosky, 1981; Rambaldi and Mo, 1984; Källén, 1981; Legras and Ghil, 1985; Tung and Rosenthal, 1985; Yoden, 1985). In

* Definition: A system is said to be in an equilibrium state if the energy associated with each and every spectral component of the solution does not change in time. This definition is physically meaningful akin to that used in statistical mechanics and is less restrictive than the notion of a purely steady state.

contrast, the dynamics of equilibria in a model without topography has received much less attention. Wiin-Nielsen (1979) and Vickroy and Dutton (1979) used a barotropic single-wave system to investigate that problem. Those studies revealed that multiple equilibria are possible in the context of such an idealised model. A sample of other related references can be found in M85. It is worth mentioning that there are some very recent high resolution numerical models to study baroclinic instability at large supercriticality (e.g., Chou and Loesch, 1986; Kline and Pedlosky, 1986).

The initial-value approach was used in M85 to determine the asymptotic states at which a small ensemble of baroclinic waves approaches at large time. A more effective method for determining the number of equilibria and investigating their dynamics is to directly solve the corresponding set of nonlinear algebraic equations as was done by Lorenz (1963) and others. It is important to note that the equilibria in this model are not strictly steady states. Therefore, one cannot begin the analysis by simply setting the time derivatives of the governing spectral equations to zero. This is due to the fact that our beta-plane model has an intrinsic zonal symmetry. The waves in an equilibrium state must then be propagating in the zonal direction. Such phase speeds in turn must be functionally related to the amplitudes and the relative phase angles of the waves yet to be determined. Those analytic relationships are first deduced in a preliminary analysis in Section 2. That amounts to deducing in advance the dimension of the subspace associated with each kind of equilibria.

We will attempt to delineate the nature of the equilibria obtained for this model by applying the bifurcation theory. That is a theory concerned with the study of the changes in the qualitative character of the solutions, particularly the equilibrium solutions, of nonlinear systems as a parameter varies. Bifurcation points are often identified (e.g., in Vautard and Legras, 1986) on the basis of the change in the number of unstable eigenvalues obtained in a linear instability analysis of an equilibrium state as a parameter varies. To fully ascertain the character of a bifurcation point, we also need to establish the particular branches of equilibria which are associated with it. This motivates us to closely examine the structural properties of all the equilibria obtained in this analysis. The results enable us to identify those points on the parameter plane where a topologically distinct equilibrium state emerges as a parameter varies across them. In this way, we will be able to unambiguously identify the relations among all the equilibria. The results also explicitly substantiate the general notion that a symmetry-breaking does occur in the solution at a bifurcation point.

Section 3 reports the analytic solutions of the equilibria for the steady-single-wave states. Its origin and physical nature are clarified on the basis of its unique structural characteristics. Section 4 reports the numerical solutions for the equilibria of the steady-multiple-wave states. The stability properties of all the equilibria and the related energetics diagnoses are carried out in Section 5. The relations among all the equilibria from the bifurcation point of view are ascertained in Section 6. Some concluding remarks are given in Section 7.

2. Basic considerations of the analysis

Following M85, we consider a two-layer quasi-geostrophic β-plane channel model. The forcing is introduced in the form of a meridional temperature gradient, and a corresponding baroclinic shear. The dissipation is incorporated through a top and a bottom Ekman layer with an equal damping rate. We take the point of view that a difference in the viscous coefficients in the top and bottom Ekman layers is to be regarded as a complication, to be analysed after the attractors of the system with equal viscous coefficients have been thoroughly understood. The asymmetric action of differential damping is expected to retard one layer by a greater extent than the other. This should then have a greater direct impact on the evolution of the baroclinic component. A destabilizing effect on the system might be induced in addition to the normal stabilizing influence of the dissipation (Reinhold, 1986). As to what the precise consequence of asymmetric dampings on the equilibration process in this model might be, only a thorough counterpart computational analysis could reveal this.

The dynamics of the system is dictated by

5 dimensionless parameters: U, r, F, β, and γ (definitions given in M85). The two key parameters are U and r which measure the strength of the baroclinic forcing and frictional damping respectively. The other parameters are F the Froude number, β the meridional variation of the Coriolis parameter, and γ the wavenumber of the lowest zonal harmonic.

The flow field can be depicted in terms of two variables ψ and θ which respectively stand for the barotropic and baroclinic components of the streamfunction representing the departure from the imposed baroclinic flow. The governing potential vorticity equations in terms of ψ and θ are

$$\begin{aligned}&\nabla^2\psi_t + J(\psi, \beta y + \nabla^2\psi) + J(\theta - Uy, \nabla^2\theta)\\ &\quad = -r\nabla^2\psi,\\ &\nabla^2\theta_t + J(\psi, \nabla^2\theta) + J(\theta, \beta y + \nabla^2\psi)\\ &\quad + J(-Uy, \nabla^2\psi) - 2F[\theta_t + J(\psi, \theta - Uy)]\\ &\quad = -r\nabla^2\theta. \end{aligned} \tag{2.1}$$

A spectral version of this model consisting of only one wave-triad and one zonal component is analysed in this study. The basis functions used for the spectral representation of the solution are

$$\begin{aligned}S_{m,n} &= \sqrt{\gamma}\,\pi^{-1}\,e^{im\gamma x}\sin ny,\\ C_{0,1} &= \sqrt{\gamma}\,\pi^{-1}\cos y,\end{aligned} \tag{2.2}$$

with $(m,n) = (\pm 1, 1)$, $(\pm 1, 2)$ and $(\pm 2, 1)$. The eigenvalue associated with the basis functions is $\lambda_{mn} = (\gamma m)^2 + n^2$. It is pertinent to first note that the two necessary conditions for the instability of an infinitesimal wave with wavenumber (m,n) are (Pedlosky, 1970)

$$\lambda_{mn} < 2F, \tag{2.3}$$

$$U^2 > U_c^2 = \frac{1}{2F - \lambda_{mn}}\left(\frac{F^2\beta^2}{\lambda_{mn}(F+\lambda_{mn})^2} + \frac{r^2\lambda_{mn}}{(\gamma m)^2}\right). \tag{2.4}$$

Furthermore, the marginally neutral wave has a frequency equal to

$$\Omega_{mn} = \beta\gamma m/(F + \lambda_{mn}), \tag{2.5a}$$

and a relative phase angle

$$\phi_{mn} = \tan^{-1}\left(\frac{r\lambda_{mn}(F+\lambda_{mn})}{\beta F\gamma m}\right). \tag{2.5b}$$

The energetics of a neutral wave is described by

$$4FU_c\gamma m\sin\phi_{mn} = 2r\lambda_{mn}\left(R_{mn} + \frac{1}{R_{mn}}\right). \tag{2.5c}$$

The ratio of the amplitude of the barotropic component to that of the baroclinic component of the (m,n) wave is R_{mn}. It is uniquely given by the corresponding eigenfunction. We will consider the same values for the Froude number ($F = 2.8$) and the beta parameter ($\beta = 10$) as in M85. We set γ equal to 1 in this study for the purpose of investigating the synoptic scale waves. It follows that the three waves retained in our spectral truncation are the only 3 possible unstable waves.

The set of spectral equations was given in (A.5) of M85 which are symbolically indicated below for ease of reference

$$\dot{X}_j = F_j(X), \quad j = 1, \ldots, 7, \tag{2.6}$$

where X stands for the seven unknown spectral coefficients $(X_1, \ldots, X_7)$, which are greater than those in M85 by a constant factor of $\pi/\sqrt{\gamma}$. The zonal component is X_1. The barotropic components of the three waves are X_2, X_4, and X_6 and the corresponding baroclinic components are X_3, X_5, and X_7. The seven known functions F_j have quadratic nonlinearity arising from the different advective processes. One unknown, X_1, is real and the remaining 6 unknowns are complex variables. (2.6) therefore effectively consists of 13 equations for 13 real variables.

We will seek to algebraically solve (2.6) for the equilibria. Obviously, there is the null solution, $X_j = 0$ for any combination of r and U. It corresponds to the so-called "Hadley solution" in Lorenz (1963). This is the only strictly steady solution in view of the intrinsic zonal symmetry of the model. In addition, there are solutions consisting of waves with time-invariant amplitudes and phases steadily propagating in the zonal direction. To facilitate a discussion on the intrinsic mathematical character of that class of solutions here, let us momentarily consider the solution for the wave components in a polar form as

$$X_j = A_j\exp(\sqrt{-1}(\Omega_j t + Q_j)), \quad \text{for } j = 2, \ldots, 7, \tag{2.7}$$

where A_j, Ω_j and Q_j are real constants with A_j being the amplitudes, Ω_j the frequencies and Q_j

the phase angles of the components of the waves. In addition, we have a zonal component X_1. Note that these quantities altogether constitute 19 unknowns. They cannot all be independent since there are only 13 degrees of freedom in the model. The zonal homogeneity of the problem implies no dependence of the equilibrium solution on the absolute value of the phase angles. Therefore, Q_2 and Q_4 may be assigned a zero value without loss of generality provided that Q_3 and Q_5 are interpreted as the relative angles between the two components of each of the $(m, n) = (1, 1)$ and $(1, 2)$ waves. We may do so because the wave-zonal flow interaction only depends on the relative angle between the barotropic and baroclinic component of each wave. The wave-wave interaction on the other hand depends also upon the relative phase among the three waves involved. We may express the additional relative phase angle as the relative phase angle among either the barotropic or the baroclinic components. It follows that we cannot further set either Q_6 or Q_7 to zero. Q_6 now is a measure of the relative angle among the three barotropic components and $(Q_7 - Q_6)$ is a measure of the relative angle between the two components of the (2, 1) wave. In other words, there must be four independent relative phase angles in an M-state. Being a measure of the intensity of the spectral components, X_1 and A_j $(j = 2, \ldots, 7)$ should be independent variables in general. The quantities considered up to this point add up to 11 degrees of freedom. It follows that only two of the six frequencies Ω_j can be independent. Indeed, upon substituting (2.7) into (2.6), one would readily find that an M state solution is necessarily characterized by

$$\Omega_{j+1} = \Omega_j, \quad j = 2, 4, 6, \tag{2.8a}$$

and the sum of the two independent frequencies of the waves must be equal to the third frequency, e.g.,

$$\Omega_2 + \Omega_4 = \Omega_6. \tag{2.8b}$$

These relations simply mean that the barotropic and baroclinic components of each wave must propagate at the same speed and that the wave-triad must be a resonant triad if the flow is to be an M-state. The relations (2.8) are indeed satisfied by the numerical solutions of M85. It is important to note that the two designated independent frequencies, say Ω_2 and Ω_4, are not coordinates of the phase space. Hence, a set of the M states constitute a subspace of only 11 dimensions. The evolution of the flow towards a stable M-state may then be visualized as a trajectory in the 13-dimensional phase space progressively approaching towards an 11-dimensional attractor.

It is algebraically simpler to seek the equilibria solutions in a Cartesian instead of a polar form. The reasoning above suggests that we may set the imaginary part of X_2 and X_4 to be zero without loss of generality and at the same time may introduce two unknown independent frequencies, say Ω_2 and Ω_4 for the solution. Hence, we may write an equilibrium solution in the form of

$$\begin{aligned} X_1 = Y_1, \quad (X_2, X_3) &= (Y_2, Y_3 + iZ_3) \exp(i\Omega_2 t) \\ (X_4, X_5) &= (Y_4, Y_5 + iZ_5) \exp(i\Omega_4 t) \\ (X_6, X_7) &= (Y_6 + iZ_6, Y_7 + iZ_7) \\ &\quad \times \exp(i(\Omega_2 + \Omega_4) t), \end{aligned} \tag{2.9}$$

where $i = \sqrt{-1}$. The space of the equilibria is then defined by the constant values of 11 real variables (Y_j $(j = 1, 7)$, Z_j $(j = 3, 5, 6, 7)$). To obtain the governing equations for them, we first equate the real and imaginary parts on both sides of (2.6) individually. Two of those 13 equations are expressions relating the frequencies Ω_2 and Ω_4 to the other 11 unknowns themselves. The resulting equations, with the substitution of the auxiliary relations, may be symbolically referred to as

$$\dot{\xi}_k = 0 = G_k(\xi) \quad \text{for } k = 1, \ldots, 11. \tag{2.10}$$

The unknowns are denoted in a vectorial form as $\xi = (Y_1, \ldots, Y_7, Z_3, Z_5, Z_6, Z_7)$ and G_k are nonlinear algebraic equations.

A special case of an M-state is a steady single-wave state (an S_{mn} state) in which two of the waves have zero amplitude. It would be meaningless in this case to assign any value for the phase angle or frequencies for those two waves. It follows that while condition (2.8a) must be still satisfied by the remaining wave, (2.8b) becomes irrelevant. Since there is only one surviving wave in this special case, we may set Z_6 to zero as well. Each set of S_{mn} states only occupies a 4-dimensional subspace. Specifically, an S_{11} state is characterized by the values of the variables

(Y_1, Y_2, Y_3, Z_3), a S_{12} state by (Y_1, Y_4, Y_5, Z_5) and an S_{21} state by (Y_1, Y_6, Y_7, Z_7).

It should be emphasized that an S_{mn} state has one frequency and therefore strictly speaking represents a limit cycle, albeit an especially simple kind since the amplitude of the wave does not change in time. On the other hand, an M-state has 2 independent frequencies. It therefore may be geometrically thought of as a 2-torus with 11 dimensions (Lanford, 1981).

3. The 4-D equilibria (the S_{mn} states)

3.1. Analytic solution

This section reports an analytic method for determining the S_{mn} states. It is exemplified by an application to the case of the S_{11} state described below. The values of the (1, 2) and (2, 1) waves are set to zero in this case. The governing equations of the remaining 5 variables in (2.9) can be readily obtained from (2.6) as

$$0 = \varepsilon_{11} Y_1 - 2\beta_{12} Y_2 Z_3 \tag{3.1}$$

$$0 = \varepsilon_{21} Y_2 - \beta_{22} Z_3 - \beta_{24} Y_1 Z_3 \tag{3.2}$$

$$\Omega_2 Y_2 = \beta_{21} Y_2 + \beta_{22} Y_3 + \beta_{24} Y_3 Y_1 \tag{3.3}$$

$$-\Omega_2 Z_3 = \varepsilon_{32} Y_3 - \beta_{32} Z_3 \tag{3.4}$$

$$\Omega_2 Y_3 = \beta_{31} Y_2 + \beta_{32} Y_3 + \varepsilon_{32} Z_3 + \beta_{35} Y_2 Y_1, \tag{3.5}$$

where

$$\varepsilon_{11} = -r\lambda_{01}/(2F + \lambda_{01}), \quad \varepsilon_{21} = -r,$$

$$\varepsilon_{32} = -r\lambda_{11}/(2F + \lambda_{11}), \quad \beta_{12} = 2F\Delta/(2F + \lambda_{0,1}),$$

$$\beta_{21} = \gamma\beta/\lambda_{11}, \quad \beta_{22} = -U\gamma,$$

$$\beta_{24} = \Delta(-\lambda_{11} + \lambda_{01})/\lambda_{11},$$

$$\beta_{31} = U\gamma(2F - \lambda_{11})/(2F + \lambda_{11}),$$

$$\beta_{32} = \beta\gamma/(2F + \lambda_{11}),$$

$$\beta_{35} = \Delta(-\lambda_{11} + \lambda_{01} + 2F)/(2F + \lambda_{11}),$$

$$\Delta = 8\gamma^{3/2}/3\pi^2.$$

We first obtain the following relations from the equations above expressing each of Y_j in terms of Z_3.

$$Y_1 = 2\beta_{12}\beta_{22}(Z_3)^2/(\varepsilon_{11}\varepsilon_{21} - 2\beta_{12}\beta_{24}(Z_3)^2) \tag{3.6}$$

$$Y_2 = \varepsilon_{11}\beta_{22} Z_3/(\varepsilon_{11}\varepsilon_{21} - 2\beta_{12}\beta_{24}(Z_3)^2) \tag{3.7}$$

$$Y_3 = (\beta_{32} - \beta_{21}) Z_3/(\varepsilon_{21} + \varepsilon_{32}). \tag{3.8}$$

Substituting (3.8) into (3.4) would give

$$\Omega_2 = (\varepsilon_{32}\beta_{21} + \beta_{32}\varepsilon_{21})/(\varepsilon_{21} + \varepsilon_{32}). \tag{3.9}$$

(3.8) immediately yields the result for the relative phase angle as

$$Q_3 = \tan^{-1}(Z_3/Y_3)$$

$$= \tan^{-1}((\varepsilon_{21} + \varepsilon_{32})/(\beta_{32} - \beta_{21})). \tag{3.10}$$

(3.9) and (3.10) can be explicitly rewritten in terms of the model parameters as

$$\Omega_2 = \beta\gamma/(F + \lambda_{11}), \tag{3.11}$$

$$Q_3 = \tan^{-1}(r\lambda_{11}(F + \lambda_{11})/(\beta\gamma F)). \tag{3.12}$$

Since all parameters appearing on the RHS of (3.11) have positive values, we conclude that the frequency Ω_2 must have positive values indicating that the wave is westward propagating as a Rossby wave must be. The RHS of (3.11) and (3.12) are identical to the corresponding properties of the neutral wave in a linear instability analysis (2.5a) and (2.5b). This is not a mere coincidence. Its implication will be elaborated upon in Subsection 3.4.

We next make use of (3.6), (3.7), (3.8) and (3.9) to rewrite (3.5) in terms of Z_3 alone. The resulting equation is a quartic equation for Z_3 as

$$(Z_3)^4 + 2s(Z_3)^2 + h = 0, \tag{3.13}$$

where

$$s = \frac{\varepsilon_{21}\varepsilon_{11}}{2\beta_{12}\beta_{24}}\left[-1 + \frac{\beta_{22}(\beta_{35}\beta_{22} - \beta_{31}\beta_{24}}{2\varepsilon_{21}\varepsilon_{32}\beta_{24}(1 + c^2)}\right], \tag{3.14a}$$

$$h = \left(\frac{\varepsilon_{21}\varepsilon_{11}}{2\beta_{12}\beta_{24}}\right)^2\left[1 + \frac{\beta_{22}\beta_{31}}{\varepsilon_{21}\varepsilon_{32}(1 + c^2)}\right], \tag{3.14b}$$

$$c = (\beta_{32} - \beta_{21})/(\varepsilon_{21} - \varepsilon_{32}). \tag{3.14c}$$

The solution for $(Z_3)^2$ is then

$$(Z_3)^2 = -s \pm \sqrt{(s^2 - h)}. \tag{3.15}$$

(3.15) together with (3.6), (3.7) and (3.8), constitute a complete analytic solution. Similar results for the other two S_{mn} states have been obtained.

3.2. Existence and uniqueness of the viscous solution

By the definition of the β's, we may rewrite

$$\beta_{35}\beta_{22} - \beta_{31}\beta_{24} = -\frac{U\gamma\lambda_{01}\Delta}{\lambda_{11}(2F+\lambda_{11})}(2F+\lambda_{11}-\lambda_{01}). \quad (3.16)$$

The RHS is negative definite. Since ε_{11}, ε_{21}, ε_{32}, β_{22}, β_{24} are all negative, and β_{12} is positive, it follows from (3.14a) in conjunction with (3.16) that s is positive definite. This fact in turn implies that a nontrivial S_{mn} state could not exist unless h is negative in view of (3.15). This necessary and sufficient condition, according to (3.14b), in turn amounts to be

$$1 + \beta_{22}\beta_{31}\Big/\left\{\varepsilon_{21}\varepsilon_{32}\left[1+\left(\frac{(\beta_{32}-\beta_{21})}{(\varepsilon_{21}+\varepsilon_{32})}\right)^2\right]\right\} < 0. \quad (3.17)$$

When written explicitly, (3.17) is equivalent to

$$U^2 > \frac{1}{(2F-\lambda_{11})} \times \left[F^2\beta^2/(\lambda_{11}(F+\lambda_{11})^2) + \frac{r^2\lambda_{11}}{\gamma^2}\right]. \quad (3.18)$$

The RHS of (3.18) is precisely identical to the baroclinic shear required for supporting a neutrally stable (1, 1) wave in a linear instability analysis, (2.3). Therefore, there cannot be a finite amplitude steady single-wave state unless the imposed baroclinic shear U exceeds the marginal value for linear instability of that wave to begin with. Baroclinic instability then belongs to the category known as "supercritical instability". The emergence of an S_{mn} state gives rise to a symmetry-breaking of the system with respect to the Hadley state (the null solution). Since an S_{mn} state has a finite frequency, we may conclude that $U = U_c$ is a Hopf bifurcation point. This interpretation is consistent with the fact that a linear instability analysis of the Hadley state yields a pair of complex eigenvalues.

When the condition (3.18) is satisfied, we have $W \equiv (Z_3)^2 > 0$ and thus $Z_3 = \pm\sqrt{W}$. According to (3.7) and (3.8), both Y_2 and Y_3 have the same sign as Z_3. It follows that either sign of Z_3 would imply the same relative angle between the barotropic and baroclinic components of the wave. The amplitude of the wave and the value of the zonal component are also independent of the sign of Z_3. Therefore, using either sign for Z_3, we would still obtain a physically identical solution of Y_j from (3.6), (3.7) and (3.8). The steady single-wave state is then unique, implying that a single-wave system would evolve towards it from any initial state. This is true as long as the model has a finite dissipation.

3.3. Structure of the 4-D equilibria

All parameters appearing on the RHS of (3.12) have positive values. It follows that Q_3 must have a value between 0 and 90 degrees. A positive value of Q_3 means a vertical westward tilt of the wave's structure in the physical space for the case of $U > 0$. The larger this angle is, the more efficient it would be as far as extracting energy from the imposed shear is concerned. It is also noted that the vertical tilt of the wave Q_3 increases with the friction but is independent of the imposed baroclinic shear. Hence, the efficiency of this wave is only dependent on the friction parameter. The counterpart results for the S_{12} and S_{21} states (Q_5 and Q_7) are qualitatively similar. The dependence on the wavenumber (m, n) is such that the values for Q_3, Q_7 and Q_5 are in increasing order, e.g., $Q_3 = 3.92$, $Q_5 = 15.57$, and $Q_7 = 7.93$ for $r = 0.2$, $F = 2.8$, $\beta = 10$, and $\gamma = 1$.

Some of the analytic results for the amplitudes of the waves for each of the S_{mn} states will be shown and discussed in Section 6 in conjunction with other results. It suffices to mention here that the amplitude is weakly dependent on the friction parameter r. This is particularly so for the (1, 1) and (2, 1) waves. The amplitudes of the S_{mn} states increase monotonically with the baroclinic forcing. The amplitudes of the (1, 1) wave are larger than those of the (1, 2) wave which are in turn larger than those of the (2, 1) wave. Furthermore, the barotropic component of the wave has a considerably larger amplitude than the baroclinic component. Y_1 is found to have a negative value.

3.4. Physical character of the S_{mn} states

A physical account of the solution of an S_{mn} state rests upon a satisfactory explanation as to why its structure is what it is. Specifically, why is the relative angle of the wave in a S_{mn} state exactly equal to that of a neutral infinitesimal

perturbation (m,n) wave? Why does the reduction of the baroclinic shear due to the wave-zonal flow interaction have a certain particular value? A pertinent fact to note is that the phase angle of an unstable perturbation for a given $U > U_c$ is greater than that for a neutral perturbation, e.g., $90° > \phi > \phi_{mn}$. The value of ϕ_{mn} may be interpreted as the minimum relative angle the (m,n) wave has to have in order to maintain itself against the frictional dissipation. The feedback of the wave-zonal flow interaction during the evolution towards an S_{mn} state tends to reduce the relative phase angle until it reaches its smallest possible value. Even when ϕ is reduced to ϕ_{mn}, the wave still extracts more energy from the imposed baroclinic shear than a linearly neutral wave does because $U > U_c$. This is required for maintaining the zonal component Y_1 against dissipation. Y_1 is a measure of a modification of the zonal baroclinic shear of which the meridional average is given by

$$\tilde{U} = U + \frac{2}{\pi^2} Y_1. \tag{3.19}$$

The energetics of an S_{mn} state are described by, according to eqs. (13), (14) and (15) of M85 written in a general form,

$$4F\gamma m U_{eqv} \sin Q_{mn} = 2r\lambda_{mn}\left(R_{mn} + \frac{1}{R_{mn}} \right) \tag{3.20}$$

$$4F\gamma m(U - U_{eqv}) R_{mn} \sin Q_{mn} = r\lambda_{01} \frac{Y_1^2}{|\theta_{mn}|^2}, \tag{3.21}$$

where

$$U_{eqv} = U + \frac{8\gamma^{1/2} n^2}{(4n^2 - 1)\pi^2} Y_1, \tag{3.22}$$

$$Q_{mn} = \phi_{mn}$$

given by (2.5b), with R_{mn} being the ratio of the amplitude of the barotropic component $|\psi_{mn}|$ to that of the baroclinic component $|\theta_{mn}|$ of the wave. Comparing (3.20) with (2.5c), we see that U_{eqv} plays the same role as U_c does. Hence, U_{eqv} is referred to as an equivalent baroclinic shear which is not numerically equal to $\tilde{U}$. We attempt to interpret the wave in a S_{mn} state as a dynamically neutral wave. This attempt is motivated by Reinhold's (1986) recent success in showing a structural determinism in the evolution of a single wave. His finding is rather remarkable since it was deduced in the context of linear dynamics of the wave. Nevertheless, our proof of existence and uniqueness of the nonlinear S_{mn} state is fully compatible with Reinhold's conclusion. To unequivocably prove our point, we have also carried out a normal mode linear instability analysis with our model for a prescribed baroclinic shear equal to $U + (Y_1/\pi)\sin y$. The procedure is straightforward. It can be readily shown that in order for this flow to be dynamically neutral, Y_1 must have a value such that the following criterion is satisfied.

$$U^{(1)} U^{(2)} = U_c^2, \tag{3.23}$$

where U_c is given by (2.4),

$$U^{(1)} = U + \frac{8\gamma^{1/2} n^2(\lambda_{mn} - \lambda_{01})}{\pi^2(4n^2 - 1)\lambda_{mn}} Y_1, \tag{3.24}$$

$$U^{(2)} = U + \frac{8\gamma^{1/2} n^2(2F - \lambda_{mn} + \lambda_{01})}{\pi^2(4n^2 - 1)(2F - \lambda_{mn})} Y_1. \tag{3.25}$$

(3.23) is a quadratic equation for Y_1. After some algebra, one can show that the permissible root of Y_1 is exactly the same as the analytic solution of Y_1 obtained before. The correct solution of Y_1 therefore can be determined via two completely different routes. One is the direct method used in Subsection 3.1. The other is based on Reinhold's idea of structural determinism. Indeed, the relative phase angle of the neutral wave is the same as our previous analytic results. The absolute values of the amplitudes of such a perturbation neutral wave can be determined on the basis of the energy balance requirements (3.20) and (3.21). The solution is therefore completely unique as found before.

One relatively minor difference between Reinhold's estimate for U_{eff} and our U_{eqv} should be noted. Reinhold's (1986) expression for the (1, 1) wave is equal to our expression $U^{(1)}$ above. Since Y_1 is negative, we have $U_{eff} = U^{(1)} > U_{eqv} > U^{(2)}$. Reinhold's result then actually corresponds to the upper bound of the range in which U_{eqv} lies. We feel that U_{eqv} is a more physically interpretable quantity than U_{eff} since it is defined on the basis of the energy balance requirement for the finite amplitude wave.

3.5. Non-uniqueness of the inviscid solution

The inviscid case ($r = 0$) warrants a separate consideration. If the solution in this case were in

the form of (2.9), the corresponding Z_3 would have to be zero according to (3.12). If so, eqs. (3.1), (3.2) and (3.4) would be automatically satisfied. Then there would only be two governing equations left, (3.3) and (3.5), for the remaining four unknowns (Y_1, Y_2, Y_3, Ω_2). It follows that such solution could not be unique in the inviscid case. This mathematical consequence might at first appear to be puzzling. But all it is trying to tell us is that the actual solution in the inviscid case need not be in the form of (2.9) in general. The physical basis of that is not hard to see. Under the inviscid condition, there is no net loss of energy from the system. Then there must not be any net conversion of energy from the zonal flow to the wave either. Of course, one possibility is to have $Z_3 = 0$, but if so some of the other variables may have arbitrary values as we have seen above. The requirement of no net energy conversion is a weak constraint and can be also met in a solution that has a periodic reversible exchange of energy between the wave and the zonal flow. Hence setting the solution in the form of (2.9) a priori would be unnecessarily restrictive. What actually happens in this special case is that the equilibrated state is a steady one only if the initial state itself happens to be a neutrally stable one with a phase angle $\Omega_3 = 0$. But the wave in such an equilibrated state could have any amplitude that we care to choose for the initial state. It is in this sense that the solution is indeterminate. In general, we should expect that Z_3 itself may vary periodically with time, signifying a reversible exchange of energy between the wave and the zonal flow. The correct solution is then a simple vacillation instead of a steady state. A sample solution of that has been given in Fig. 2 of M85. The interpretations above concerning the inviscid solutions are also in agreement with those of Reinhold (1986).

4. The 11-D equilibria (the M states)

These attractors are the solutions of (2.10), obtained with the use of a modified Newton's method (the "hybrid-method", Powell, 1970). Our numerical computations have uncovered the existence of two distinct families of M states which are referred to as the MA and MB states. Each of these M states is found to exist only in a part of the parameter region that we have carefully scanned through ($0 < r \leqslant 0.5$ and $2.0 \leqslant U \leqslant 5.0$). The regions for the existence of the MA and MB states are nevertheless quite extensive, with a substantial overlap between them. Extensive numerical experimentations did not yield additional multiple wave states.

The MB state is a newly discovered class of equilibrium solutions, which exists only for small to moderate friction, $0 < r \leqslant 0.4$. Fig. 1 shows the results of the amplitude components of its three equilibrated waves. They mainly increase with the forcing intensity and have weak dependence on the friction. Fig. 2 shows the results of the four independent relative phase angles and those of the two independent frequencies, Ω_3 and Ω_7. The phase angles (see Section 2 for their definitions) vary mainly with the friction parameter and only weakly vary with the forcing parameter. It should be noted that the relative angle of the (2, 1) wave, Q_7–Q_6, is an exception. It has a negative value for large U ($U > 3.0$), implying that this wave gives up some energy to the imposed zonal flow. In contrast to the frequency of an S_{mn} state as given in (3.11), its two frequencies do vary with both friction and forcing. Both frequencies increase strongly with the forcing. The dependence on friction is somewhat weaker. The only quantity not shown here is the value of the zonal component which is negative everywhere and has a similar dependence on the parameters as A_2 shown in Fig. 1a.

The MA states exist only for small to moderate values of the baroclinic forcing, $2.3 \leqslant U \leqslant 3.7$. The counterpart results for the MA states are not shown for brevity. The numerical values of the MA state variables for large friction are equal to those for the M-state in M85. The detail results for a representative friction, $r = 0.1$, will be shown and discussed in Section 6.

The fundamental difference between a MA and a MB state is manifested in the variations of the energetics with U. The results for $r = 0.1$ are shown in Fig. 3. They are computed with the formulas given in M85. Fig. 3a shows that the generation and dissipation rates of the energy associated with the barotropic components (G_B and D_B terms) are larger for the MB state than for the MA-state. The conversion terms C(A, Z) and C(B, Z) are not too different in the two cases. Unlike the case of the MA-state, the generation

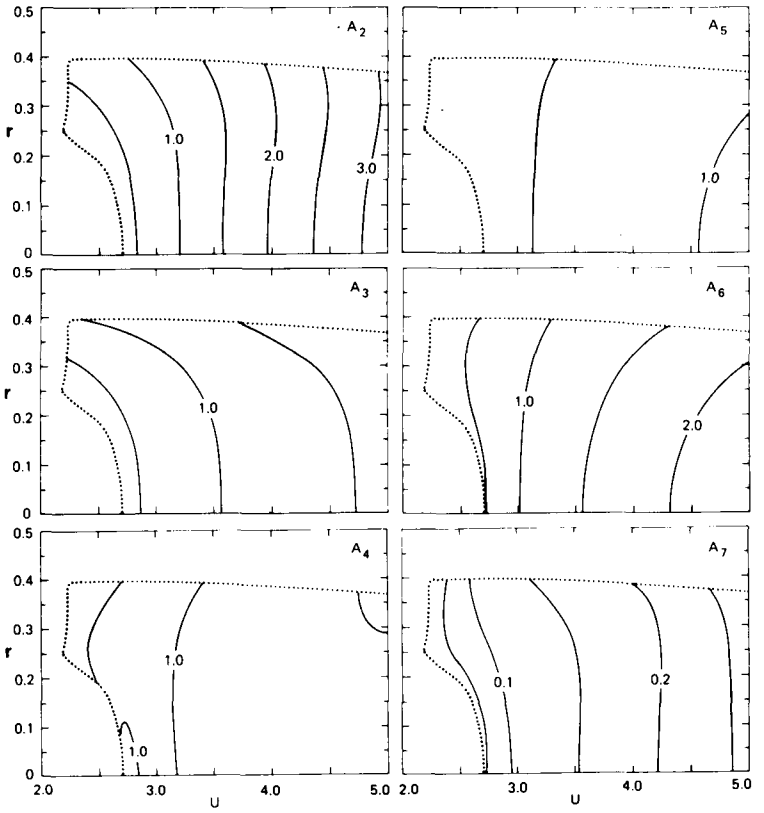

Fig. 1. Variation of the nondimensional amplitudes of the waves in the *MB*-state with the damping (r) and the forcing (U) parameters. A_2, A_4, and A_6 for the barotropic components, A_3, A_5, and A_7 for the baroclinic components.

term for the baroclinic energy is distinctly larger than the dissipation term for the *MB*-state (Fig. 3b), so that there could be a significant excess of energy for a systematic conversion from the baroclinic to the barotropic energy through the process of wave-wave interaction. This is also clearly evident in Fig. 3d where we see that the C(A, B) term is much larger for the MB state than for the *MA*-state.

5. Stability of the equilibria

Unlike Lorenz (1972), Jones (1979), and many others who analysed the instability of a free Rossby wave in the absence of forcing and damping, we analyse the stability of a wavy basic state which is itself a nonlinear solution of a forced-dissipative system. The linear stability of the S_{mn} states and the M-states need be analysed separately because the number of degrees of freedom of the perturbations in these cases are different.

5.1. *Stability of the 4-D equilibria (the S_{mn} states)*

The stability analysis of an S_{mn} state with respect to infinitesimal perturbation may be again exemplified by that of a S_{11} state. The known S_{11} state can be referred to by the form given in (2.9) with $Y_4 = Y_5 = Y_6 = Y_7 = Z_5 = Z_6 = Z_7 = 0$. The perturbation may be regarded as sufficiently small so that the part of the perturbation containing the variables of the attractor has the same dimension as that of the attractor itself, namely four. Hence, we should be dealing with a perturbation with only 12 degrees of freedom. The perturbation variables are denoted

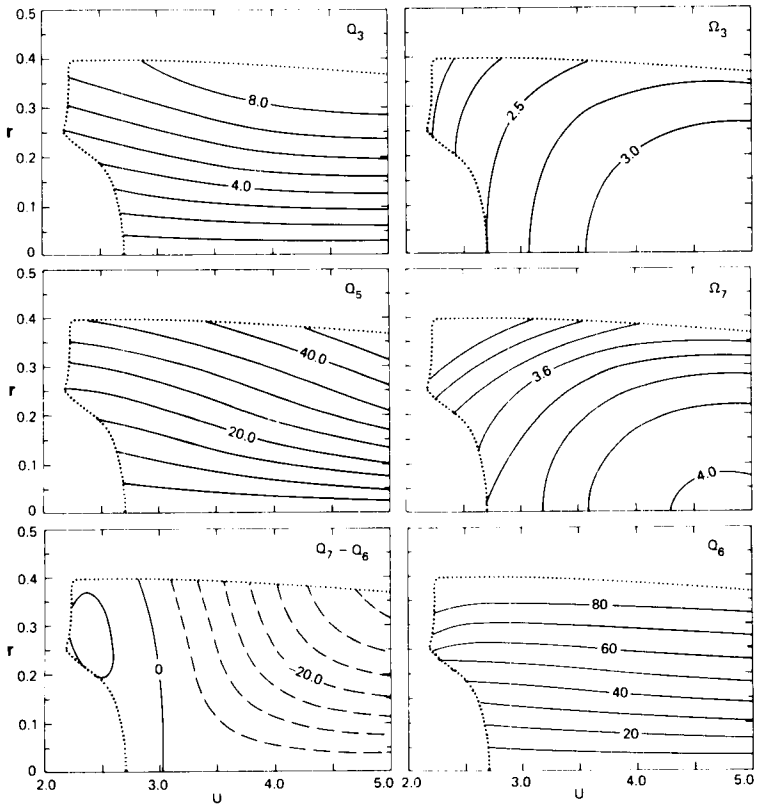

Fig. 2. Variation of the different relative phase angles (Q_3, Q_5, Q_7–Q_6, and Q_6) in degrees and of the two independent nondimensional frequencies (Ω_3, Ω_7) of the waves in the MB state with r and U.

by the corresponding letters of lower case y_j and z_j ($j = 1, \ldots, 7$ with $z_1 = z_2 = 0$) which are unknown functions of t. The total variables are defined as

$$X_1 = Y_1 + y_1$$

$$(X_2, X_3) = (Y_2 + y_2, Y_3 + iZ_3 + y_3 + iz_3) \exp(i\omega t)$$

$$(X_4, X_5) = (y_4 + iz_4, y_5 + iz_5) \exp(-\omega t)$$

$$(X_6, X_7) = (y_6 + iz_6, y_7 + iz_7),$$

with

$$\omega = \Omega_2 + \frac{\beta_{24} Y_3}{Y_2} y_1 + \frac{(\beta_{21} - \Omega_2)}{Y_2} y_2 + \frac{(\beta_{22} + \beta_{24} Y_1)}{Y_2} y_3. \quad (5.1)$$

The expression for ω is the linearized form of the frequency associated with the equilibrium under consideration. It is easy to show that the set of 12 linearized equations are made up of two decoupled subsets,

$$\dot{p} = Hp, \quad (5.2)$$

$$\dot{q} = Eq, \quad (5.3)$$

where p is the vector (y_1, y_2, y_3, z_3) and q is the vector $(y_4, \ldots, y_7, z_4, \ldots, z_7)$. H is a 4×4 matrix and E is an 8×8 matrix. We seek normal mode solution of both (5.2) and (5.3) in the form of $\exp(\sigma t)$. Since these two matrix equations are decoupled, we would obtain two distinct sets of eigenvalues σ.

It is found that the eigenvalues obtained from (5.2) at all parametric conditions have a negative real part implying a stability of the S_{11} state with respect to its own perturbation. This is to be expected because of the structural determinism of an S_{mn} state. In contrast, the eigenvalues obtained from (5.3) may have a positive real part, implying instability with respect to a perturbation of the

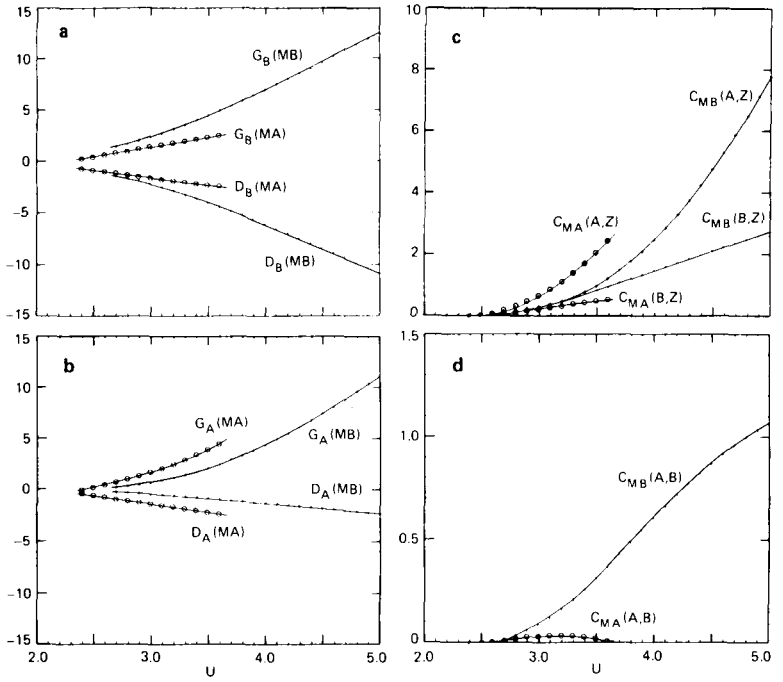

Fig. 3. A comparison of the energetics for the *MA*-states and for the *MB*-states as a function of U at $r = 0.1$ Notations: A, the wave baroclinic energy; B, the wave barotropic energy; Z, the zonal energy; $G_A(\xi)$, $D_A(\xi)$, respectively, the generation and dissipation rates of A-type energy for the ξ state; $C_\xi(A, z)$, the conversion rate from A to z for the ξ state; etc.

other two waves. Fig. 4a shows the real part of the latest eigenvalue obtained from solving (5.3) as a function of the two key parameters, r and U. The shaded area delineates the stable S_{11} states under the conditions of large dissipation and forcing. There are two pairs of unstable eigenvalues in the stippled area. The area in between has one pair of unstable eigenvalues. This information concerning the change in the number of eigenvalues will be needed in interpreting the relation among the equilibria in Section 6. For reasons to be clearer soon, the different segments of the boundary curves are labelled with Roman numerals.

The counterpart results of the linear instability analysis for the S_{12} and S_{21} states are shown in Fig. 4b and 4c. It is seen that the stable S_{12} states only exist in a small parametric region characterized by small friction and supercriticality. On the other hand, the stable S_{21} states only exist in a narrow strip of parametric conditions characterized by even smaller values of supercriticality. Friction is however not as unfavorable to the S_{21} states as to the S_{12} states. The findings concerning the regions of stable S_{mn} states are in quantitative agreement with the results reported in M85 (see Fig. 9 of M85). The magnitude of σ gives us an indication of how rapidly the system, as viewed in terms of its trajectory in the phase space, would "escape" from each of these 4-D attractors under different parametric conditions when it happens to be in one of their neighborhoods.

5.2. *Stability ot the 11-D equilibria (the M states)*

The perturbation may be assumed to have the same dimension as that of the attractor without loss of generality. The total value of the vector variable is

$$\xi = \bar{\xi} + \xi', \tag{5.4}$$

where ξ' is a perturbation which is governed by the following linearized form of (2.6) with respect to $\bar{\xi}$

$$\xi_k' = \sum_{n=1}^{11} (\partial G_k(\bar{\xi})/\partial \xi_n)\, \xi_n' \quad \text{for } k = 1, \ldots, 11. \tag{5.5}$$

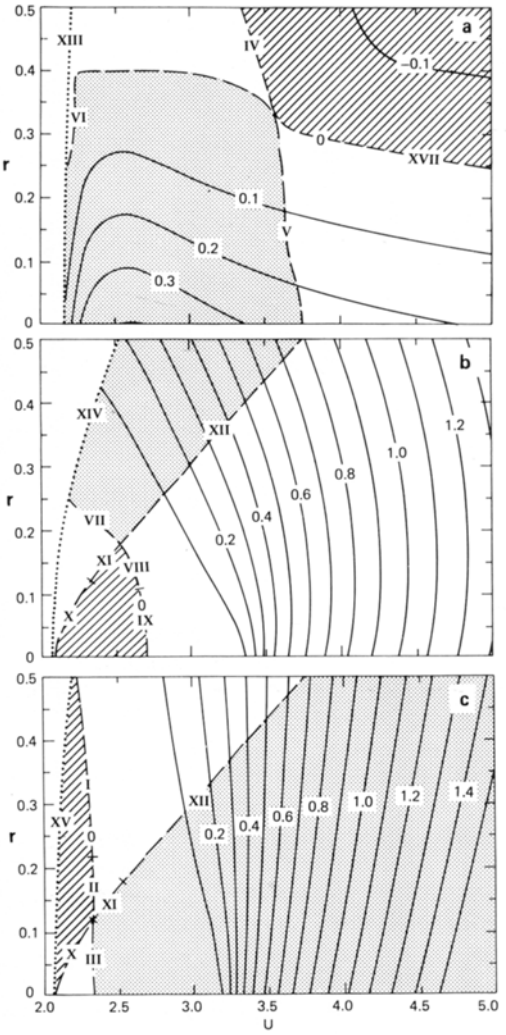

Fig. 4. Variations of the largest real part of the eigenvalue for the S_{mn} states with r and U: (a) S_{11} states, (b) S_{12} states, and (c) S_{21} states. The shaded area has no unstable eigenvalue, the stippled area has four unstable eigenvalues, and the area in between has two unstable eigenvalues. The curve segments labelled with Roman numerals are curves along which bifurcations have been identified (see text for details).

Seeking the normal mode solution to be proportional to $\exp(\sigma t)$, we would be again led to solving a simple matrix equation for the eigenvalue σ. The largest real part of the eigenvalues for the *MA*- and *MB*-states are shown in Fig. 5. The regions of the stable *MA*- and *MB*-states are shaded. The stable *MA*-states

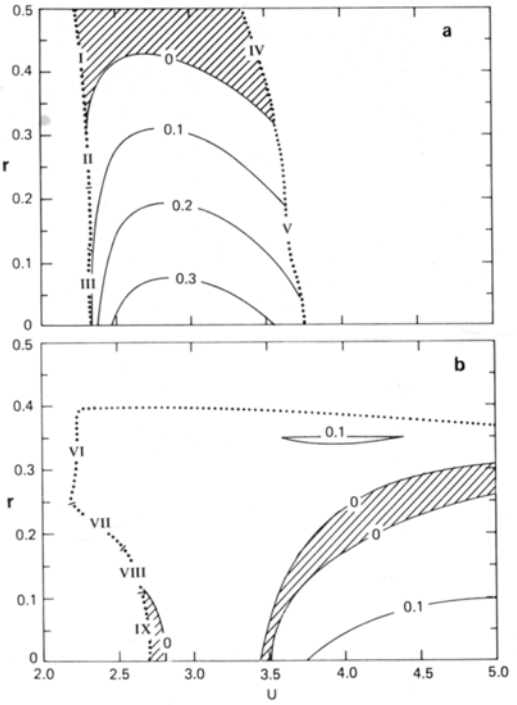

Fig. 5. Variations of the largest real part of the eigenvalue for (a) the *MA*-states and (b) the *MB*-states with r and U. The shaded area has no unstable eigenvalues. The curve segments labelled with Roman numerals are curves along which bifurcations have been identified (see text for details).

exist only for rather large values of r and moderate values of U. It would not be possible to identify the existence of unstable *MA*-states for small r by initial-value calculations. These values of the growth rate is rather modest compared to the large values in Figs. 4b and 4c. The *M*-states reported in M85 clearly correspond to the family of *MA*-states. Fig. 5b shows the existence of stable *MB*-states over 2 somewhat narrow ranges of conditions as indicated by the shaded areas. The stable *MB*-states were not detected in M85 because the initial conditions used in the time integrations were too far away from this attractor. Without prior knowledge of the structure of this equilibrium state, it would be highly unlikely for one to obtain it by that method.

The information about the number of nontrivial equilibrated states in the various parts of the parameter space is summarized in Fig. 6. It shows that there can be as many as 5 different

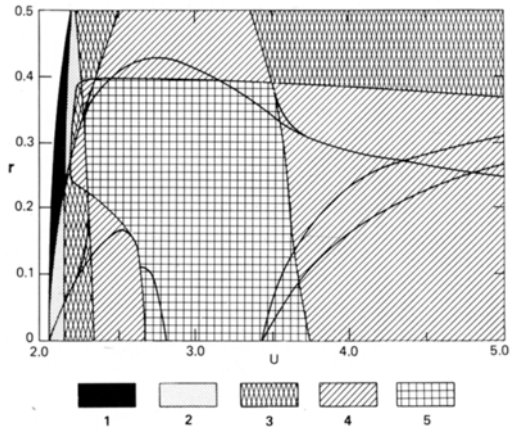

Fig. 6. Variations of the multiplicity (number) of the equilibria with r and U. The boundary curves for all the stable and unstable equilibria are also indicated for ease of reference.

equilibrated states at a given point on the (r, U) parameter plane, but there can be as few as one state. The latter is found in a narrow strip on the (r, U) plane next to the marginal instability curve for the S_{21} wave. Since the three marginal instability curves for the three waves under consideration are close to one another, the number of equilibria varies sensitively with U in the neighborhood of small supercriticality. The computations reveal that the regions of the stable S_{mn} states do not overlap, and each of them also does not overlap with the region of the stable *MA*-states. The region of the stable S_{11} state however does slightly overlap with the region for the stable *MB*-state ($0.25 < r < 0.35$, $4.7 < U \leqslant 5.0$). This is an example of an unstable baroclinic flow that has truly stable multiple equilibria.

5.3. *Energetics diagnosis of the instability*

The energy of the baroclinic components, that of the barotropic components and that of the zonal component of the equilibrated state are denoted by A, B and Z respectively as in M85 with identical definitions. By analogy, we will refer to the corresponding parts of the energy of the perturbation by the same letters in lower case, namely a, b and z. It is a straightforward matter to derive from (5.5) the governing equations for $\dot{a}$, $\dot{b}$, and $\dot{z}$. The resulting equations are written in symbolic form as follows.

$$\dot{a} = [-D_a + G_a] + [C(Z,a) + C(A,a) + C(B,a)] + C(z,a) - C(a,b), \tag{5.6}$$

$$\dot{b} = [-D_b + G_b] + [C(Z,b) + C(A,b) + C(B,b)] + C(z,b) + C(a,b), \tag{5.7}$$

$$\dot{z} = -D_z + [C(B,z) + C(A,z)] - C(z,b) - C(z,a). \tag{5.8}$$

These systematic notations should help make the physical meaning of each of the terms above self-evident. For example, a positive value of $C(B,a)$ means a conversion rate from the barotropic energy of the equilibrated multiple-wave state to the baroclinic energy of the perturbation. The explicit formulas for all the energetics terms are given in the Appendix for reference.

Each term on the RHS of (5.6), (5.7) and (5.8) has been evaluated with a normalized eigenfunction such that the total energy $(a + b + z)$ of the perturbation is equal to unity. It suffices to examine the sum of the terms in each square bracket in those equations as a single quantity. The meaning of these combined quantities is obvious. For example, a positive value of $[-D_a + G_a]$ means a net rate of increase in the baroclinic energy of the perturbation due to a generation by the imposed zonally symmetric baroclinic state in excess of the dissipation of a. For convenience a positive value of this quantity will be referred to below simply as the energy of a obtained from the imposed baroclinic state.

The energetics of the perturbations for the S_{mn} states may be regarded as a special case under consideration. Since each S_{mn} state can only be unstable with respect to perturbations in the complementary subspace (i.e., those governed by (5.3)), we only need examine the energetics for such perturbations. The results reveal that the perturbation mainly extracts energy from the imposed baroclinic state rather than from the S_{mn} state. The $C(a,b)$ term typically has a very small value. The stable perturbation mainly loses energy to the equilibrated wavy state. The details of these results are not shown for brevity.

Fig. 7a summarizes the energetics of the least stable eigenfunction for the MA state with $r = 0.45$ and $U = 2.8$. The values reveal that although the wavy basic state gives a net supply of energy to the perturbation, the imposed baroclinic state extracts energy at a greater rate from the perturbation. Furthermore, the values of

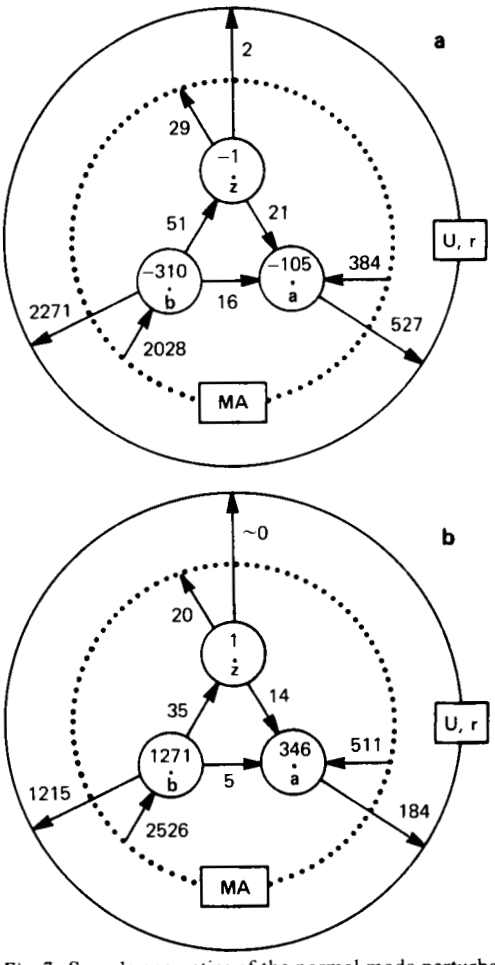

Fig. 7. Sample energetics of the normal mode perturbation with respect to the *MA*-states: (a) a stable case, $r = 0.45$, $U = 2.8$, and (b) an unstable case, $r = 0.3$, $U = 2.5$. The actual nondimensional values have been multiplied by a factor of 10^4.

the conversions among the a, b and z of this stable perturbation are found to be so small that they are of no consequence to the overall energetics. Fig. 7b shows the counterpart results of the most unstable eigenfunction for an *MA*-state with $r = 0.3$ and $U = 2.8$. Here the equilibrated wavy state is the energy source for the perturbation supplying more energy than the loss to the imposed baroclinic state.

The energetics of the normal mode perturbation for the MB states are somewhat more complicated. The complexity arises from the fact that different branches of the normal mode perturbations become unstable in different ranges of values of U and r. The variations of the real part of the eigenvalues are plotted as a function of U for $r = 0.1$ in Fig. 8. We see that the branch labelled "1" is unstable for $U < 3.60$, whereas the branch labelled "2" becomes the unstable one for $U > 3.72$. The eigenfunctions of these two branches have different structures. It follows that they have different energetics characteristics. Fig. 9a is an energetics diagram for the unstable perturbation for a MB state for $U = 3.3$ and $r = 0.1$. The normal mode belongs to the branch labelled "1" in Fig. 8. We particularly would like to draw the reader's attention to the feature that unlike for a *MA*-state $C(a, b)$ is now significant. Without the positive value of $C(a, b)$, db/dt would not be positive because the loss of barotropic energy to the imposed baroclinic state and to the zonal energy exceeds the supply from the equilibrated wavy state. The $C(a, b)$ conversion is maintained primarily by the conversion of baroclinic energy from the equilibrated wavy state. Hence, this perturbation as a whole intensifies as a result of a net energy from the equilibrated wavy state.

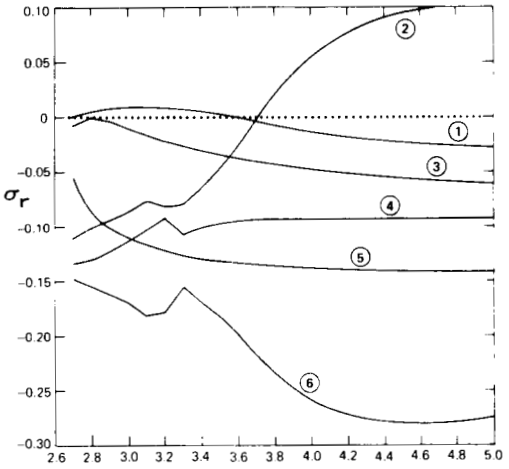

Fig. 8. Variation of the real part of the eigenvalues with respect to the *MB*-states with U for $r = 0.1$. The 6 branches of the eigenvalues are designated by the encircled numbers.

Fig. 9b is an energetics diagram for the unstable perturbation for the MB state for a larger value of U ($U = 3.8$). The unstable normal mode belongs to the branch labelled "2" in Fig. 8. Here, the imposed baroclinic state assumes the

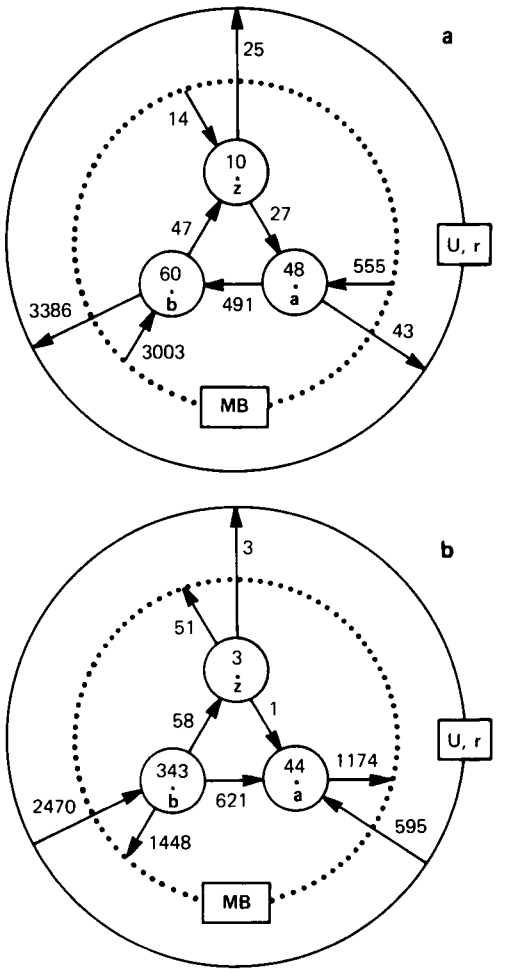

Fig. 9. Sample energetics of the normal mode perturbation with respect to the MB states: (a) an unstable case, $r = 0.1$, $U = 3.3$, and (b) also an unstable case, $r = 0.1$, $U = 3.8$.

role of an energy source, whereas the equilibrated wavy state is an energy sink. The instability results from the fact that the former supplies more energy than what is lost to the latter. The process $C(a, b)$ is important to the growth of the baroclinic energy of the perturbation in this case. Because of it, da/dt could have a positive value.

6. Equilibria from the viewpoint of bifurcation

We first seek to identify the parameter points at which the known branches of equilibria bifurcate. An elementary but pertinent geometrical consideration is that if two objects with dimensions k_1 and k_2 intersect in a space of dimension k_3, the intersection would have a dimension of $k_1 + k_2 - k_3$. When the sum of k_1 and k_2 is smaller than k_3, there is generally no intersection. Here we are considering 4-D and 11-D equilibria in a space of 13-D. An intersection can be identified from its projection on each phase space variable. Now let us closely examine how the structural properties of all equilibria vary with the parameters.

It suffices to present the variations of the equilibria with the baroclinic forcing U at a fixed value of r (say, $r = 0.1$). Fig. 10 shows the values of the zonal component X_1 of all the equilibria. All values are comparably small when U is small and therefore no definite deductions can be made from them. But Fig. 10 does clearly reveal that the *MB*- and S_{12} states bifurcate at $U \approx 2.68$ as U increases across it. The values of X_1 associated with the *MA*- and S_{11} states are quite close together. The *MA*- and S_{11} states bifurcate at $U \approx 3.69$ as U decreases across it. These two points are labelled on the U-axis as 5 and 6 respectively. The other 4 points, labelled 1 to 4, are identified on the basis of the values of the amplitudes, phase angles and frequencies of the wave components shown in Figs. 11, 12, and 13.

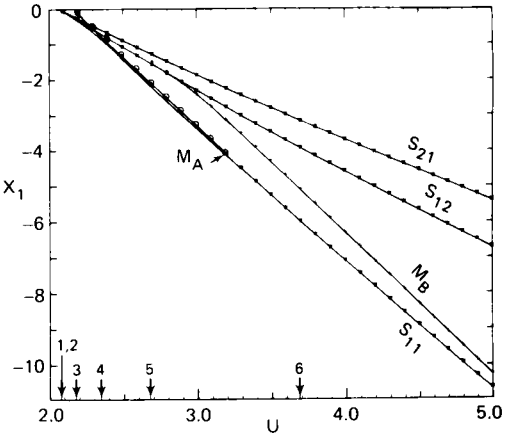

Fig. 10. A comparison of the zonal spectral coefficient, X_1, of the S_{mn}, *MA*-, and *MB*-states as a function of U for $r = 0.1$. Bifurcation points are indicated by arrows with number-labels on the U-axis. Values of U at the points 1 to 6 are 2.08, 2.09, 2.18, 2.34, 2.68, and 3.69, respectively.

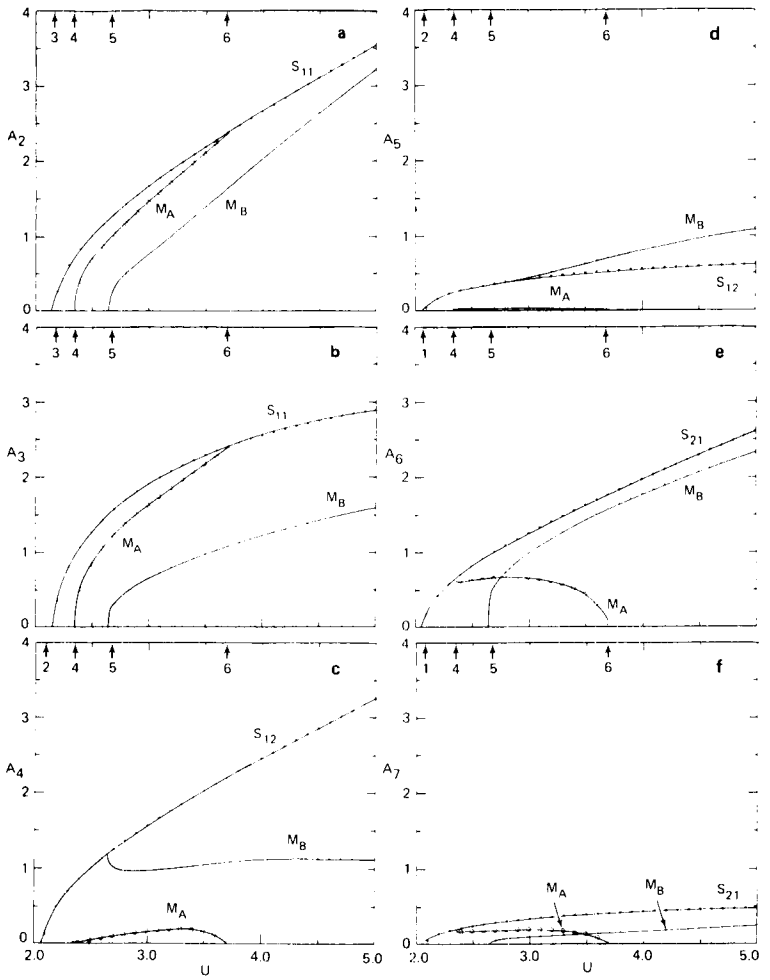

Fig. 11. A comparison of the nondimensional amplitude of the wave components of the various equilibrium states as a function of U for $r = 0.1$. Bifurcation points are indicated by arrows with number labels on the U-axis.

Fig. 11a and 11b show that the S_{11}, *MA*-, and *MB*-states emerge at $U \approx 2.18$, 2.34, and 2.68 respectively. It clearly verifies that the MA state converges to the S_{11} state at $U \approx 3.69$. These 4 points are labelled as 3, 4, 5, and 6 respectively and correspond to those points with the same labels in Fig. 10. It is clear from Fig. 11e and 11f that the *MA*-state bifurcates from the S_{21} state at $U \approx 2.34$. Thus, the *MA*-state bifurcates from a S_{21} state at $U \approx 2.34$, but it bifurcates to a S_{11} state at $U \approx 3.69$. The *MA*-state is resemblent of a S_{21} state for smaller values of U in this range, and is resemblent of a S_{11} state for larger values of U. We may therefore conclude that a *MA*-state is not fundamentally different from a S_{mn} state. Figs. 11c to 11f also show that the S_{21} state and the S_{12} state emerge at $U \approx 2.08$ and 2.09, respectively. These two points are labelled on the U-axis as 1 and 2 respectively. Figs. 11e and 11f also confirm that the MB state bifurcates from the S_{12} state at $U = 2.68$. The structure of the *MA*- and *MB*-states are distinctly different at all parameter values. They are therefore two dynamically different states as conjectured earlier on the basis of the energetics consideration. Furthermore, the MB state is different from all S_{mn} states at large values of U. This confirms that the MB state uniquely stems from the nonlinear wave-wave

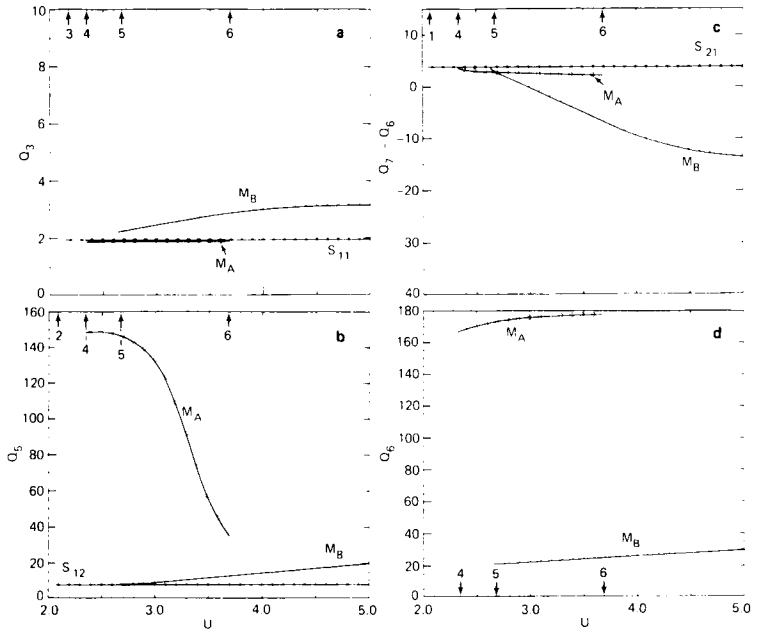

Fig. 12. A comparison of the relative phase angles in degrees associated with the various equilibrium states as a function of U for $r = 0.1$. Bifurcation points are indicated by arrows with number labels on the U-axis.

interaction which is naturally stronger for a larger forcing.

The previous deductions made on the basis of the results of the spectral amplitudes are in agreement with those deductions made on the basis of the results of the phase angles and frequencies as shown in Figs. 12 and 13. This agreement is of course not surprising, since the bifurcation of two states at a given parameter value is necessarily manifested in all structural properties of the states.

We supplement the analysis above by making use of the information about the eigenvalues obtained in the linear instability analysis of the S_{mn} states. What needs to be considered are the boundary curves of the domains for the equilibria and the curves separating the regions with different numbers of unstable eigenvalues in Figs. 4 and 5. The segments of boundaries labelled with Roman numerals in Fig. 5 correspond to those in Fig. 4. A summary of all bifurcations that can be associated with the known equilibria found in this study is given in Table 1. It is seen that the relations of the equilibria are fairly complex. The conclusions concerning the relations between the S_{21} and the

Table 1. *A summary of the bifurcations among the equilibria*

Curve segments in Figs. 4 and 5 labelled as	Bifurcation type	Change of equilibria as the baroclinic forcing increases
I	H2	$S_{21} \rightarrow MA$
II	H2	$S_{21} \rightarrow MA^*$
III	H3	$S_{21}^* \rightarrow MA^*$
IV	H2	$MA \rightarrow S_{11}$
V	H3	$MA^* \rightarrow S_{11}^*$
VI	H3	$S_{11}^* \rightarrow MB^*$
VII	H3	$S_{12}^* \rightarrow MB^*$
VIII	H2	$S_{12} \rightarrow MB^*$
IX	H2	$S_{12} \rightarrow MB$
X	H2	$S_{21} \rightarrow S_{12}$
XI	H3	$S_{21}^* \rightarrow S_{12}$
XII	H3	$S_{21}^* \rightarrow S_{12}^*$
XIII	H1	Hadley $\rightarrow S_{11}^*$
XIV	H1	Hadley $\rightarrow S_{12}^*$
XV	H1	Hadley $\rightarrow S_{21}$

Unstable equilibria are indicated by adding an asterisk. "Hadley" refers to the null state. H1 refers to a Hopf bifurcation from the Hadley state. H2 and H3 denote the Hopf bifurcations associated with a change from zero to two unstable eigenvalues, and from two to four unstable eigenvalues for a S_{mn} state respectively.

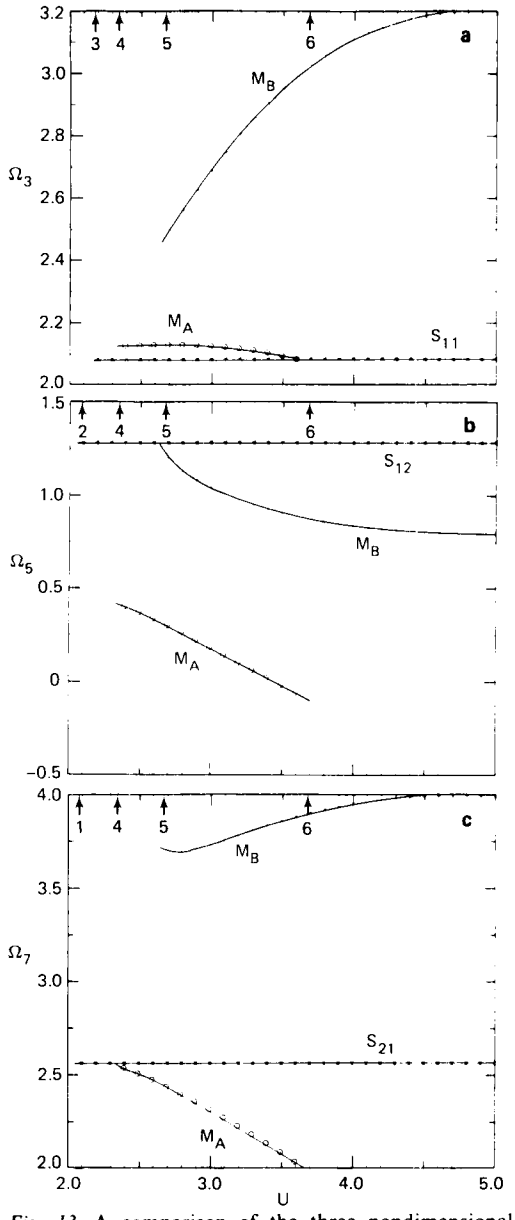

Fig. 13. A comparison of the three nondimensional frequencies associated with the various equilibrium states as a function of U for $r = 0.1$. Bifurcation points are indicated by arrows with number labels on the U-axis.

S_{12} states is made on the basis of the finding that there is an increase of two unstable eigenvalues for the S_{21} states along the curve segments X, XI, and XII and a corresponding decrease of two unstable eigenvalues for the S_{12} states. The conclusions deduced from the structural properties are in complete agreement with those made on the basis of the eigenvalues.

Fig. 14 is a concise, although less detailed, graphical summary of the relations among all the equilibria for $r = 0.1$. The sense of the changes among the equilibria is depicted by the arrows in Fig. 14 as U increases. The 3 axes are labelled as E_{11}, E_{12}, and E_{21}. Each point on the axis E_{mn} represents a S_{mn} state, quantitatively measured by the sum of the amplitude of barotropic and baroclinic components of the corresponding wave (e.g., $A_2 + A_3$ for the E_{11} axis). The stable equilibria are depicted with thick line segments and the unstable ones with thin line segments. One three-dimensional curve labelled E_A represents the unstable MA states at different values of U. The 3 dotted curves are its projections on the three planes. Another three-dimensional curve labelled E_B represents the *MB*-states. The points labelled by the numbers 1 to 6 and the

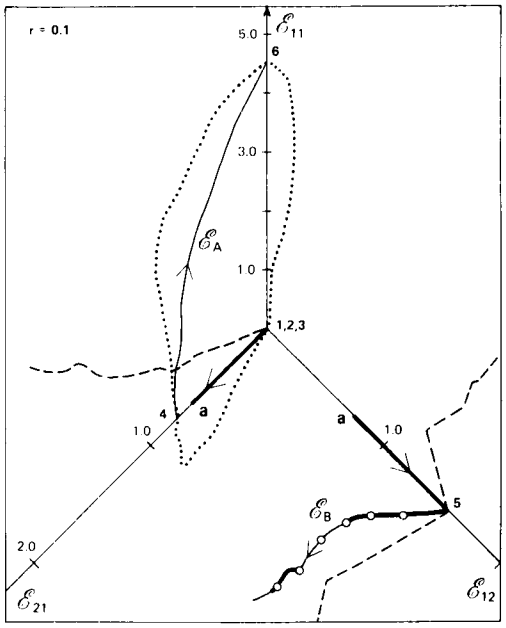

Fig. 14. A summary of the topological relations among the S_{mn}, *MA*-, and *MB*-states for weak friction, $r = 0.1$. See the text for the details of the notations (heavy lines are stable equilibria, light lines are unstable equilibria, dotted and dashed lines are projections of the E_A and E_B curves).

letter a are bifurcation points. The value of U at the point a is 2.22.

A counterpart diagram can be readily constructed for each value of r. For moderate values of friction (e.g., $r = 0.35$), the relations among the S_{21}, MA-, and S_{11} states are qualitatively the same as those in the case of $r = 0.1$. The MA-state is now stable for some values of U near both sides of its domain of existence as can be seen from Fig. 5. The curve depicting the MB-states emanates from the E_{11} axis instead of the E_{12} axis for this value of r. The MB-state is unstable for the whole range of values of U under consideration. The counterpart diagram for a larger value of r (e.g., $r = 0.5$) is even simpler since no MB-state exists for such a large value of r. There is a stable equilibrium state for each value of U. The latter takes on the form of a S_{21} state when U is small, then it changes to a MA-state at intermediate values of U and a S_{11} state for large values of U. The precise values of U where those bifurcations occur can be found in Figs. 4a, 4c, 5.

7. Concluding remarks

Apart from the null state of no motion relative to the imposed zonal baroclinic flow (the Hadley state), we have shown that there can be in general five different equilibria in this forced dissipative model of a triadic baroclinic wave system. A slightly disturbed Hadley state could evolve to one of those states if the baroclinic forcing exceeds the corresponding marginal value. The relations among the equilibria are quite complex, but are fully understandable from the bifurcation point of view. Those findings are summarized in Table 1.

A viscous steady-single-wave state develops as a consequence of a Hopf bifurcation from the Hadley solution. A single-wave system is structurally deterministic since the structure and phase speed of an unstable wave under all initial conditions must inexorably evolve towards the S_{mn} state. Such a wave is dynamically neutral with respect to the modified zonal flow. An inviscid S_{mn} state is not unique and generally takes the form of a simple limit cycle. When an S_{mn} state is unstable, the perturbation is necessarily associated with the complementary subspace and extracts energy for its growth from the imposed baroclinic shear rather than from the S_{mn} state. These findings substantially extend our knowledge of the baroclinic instability of a single Rossby wave into the nonlinear regime.

We have found two distinctly different forms of multiple-wave equilibria. The MA-state is essentially a modified form of a primary single-wave state. In contrast, the MB-state is characterized by having a strong wave-wave interaction. These interpretations are in full agreement with the findings that sufficiently strong dissipation is not conducive for the MB-states, whereas sufficiently strong forcing is not favorable for the MA-states. The triad-limit-cycle could be interpreted as a manifestation of the instability of the multiple wave equilibria. We have also found a small part of the parameter domain where either a stable S_{11} state or a stable MB-state may prevail. The MA- and MB-states may be viewed as a consequence of an additional symmetry-breaking from the S_{mn} states as the forcing further increases.

To deduce all those fundamental properties of the nonlinear dynamics summarized above is the primary objective of this theoretical investigation. Completion of such a task is feasible only for a model with a modest number of spectral components. This brings up the question as to whether or not retaining only a wave triad in an analysis is meaningful. It goes without saying that this strategic choice can only be conditionally valid. We have deliberately chosen a sufficiently small Froude number such that all the truncated waves are baroclinically stable under any forcing conditions. The formulation as such is therefore consistent with the objective of determining the bifurcations associated with the instability. The adverse effect of truncation is also hopefully minimized by doing so. A separate study with a high resolution barotropic model has yielded a similar sequence of equilibria. That analysis will be reported in a separate paper. Our optimism about the qualitative validity of this relatively low-dimensional model is therefore not without substantial reasons.

Ideally, one would also like to relate the results presented here together with those reported in M85 to observation. In view of the complexity in the detailed features of typical tropospheric disturbances, it would be unlikely to document clear

evidence there. It seems more hopeful for that purpose to consider the stratospheric region where there is least complication. The main reason is that only very few waves are present there even in the active period of the year (the winter). The dominant wave motions there typically consist of zonal wavenumber 1 and/or 2. It follows that if and when the nonlinear process is important, we might find a relatively clear signature of it. Indeed, Smith (1983) and Smith et al. (1984) have reported pronounced events in the period from November 1978 to January 1979 in the stratosphere, which are highly suggestive of strong wave-wave interaction. Those enstrophy budget analyses convincingly have documented the occurrence of vacillation between waves 1 and 2, resulting primarily from the nonlinear wave-wave interaction within the stratosphere. Such an observation vacillation in a simple atmospheric setting is the clearest indication that the triadic model analysed in M85 and in this study can be geophysically relevant.

8. Acknowledgement

This research was supported by the United States National Science Foundation under grant ATM83-11175. Part of the computations were made with the computing facility at the National Center for Atmospheric Research and the National Center for Supercomputing Applications at U. of Illinois. The helpful comments from the reviewers and B. Reinhold are gratefully acknowledged. The manuscript was ably prepared by Mrs. Norene McGhiey.

9. Appendix

Energetic equations of a perturbation about an M-state

Consider a normal mode perturbation about an M state. For convenience, we use w_j ($j = 1, \ldots, 7$) and X_j ($j = 1, \ldots, 7$) to represent the perturbation variables and the M-state variables, respectively. The subscript j has the same meaning as that in (2.6). It should be noted that $\mathrm{Im}\, w_k = \mathrm{Im}\, X_k = 0$, for $k = 1$, 2 and 4. The eigenvalue associated with the normal mode is denoted by $\sigma = \sigma_r + i\sigma_i$. First, we define

$$\langle \xi \rangle = \tau^{-1} \int_0^\tau \xi \exp(-2\sigma_r t)\, \mathrm{d}t, \tag{A.1}$$

where $\tau = 2\pi/\sigma_i$. We also define,

$$\dot{a} = \langle (\mathrm{d}a/\mathrm{d}t) \rangle$$
$$\dot{b} = \langle (\mathrm{d}b/\mathrm{d}t) \rangle$$
$$\dot{z} = \langle (\mathrm{d}z/\mathrm{d}t) \rangle. \tag{A.2}$$

Based on (5.5), we may easily obtain the corresponding energetic equations, the symbolic form of which is given by (5.6)–(5.8). The explicit forms of all the terms in (5.6)–(5.8) are as follows.

$$D_a = 2r\langle (\lambda_{11}|w_3|^2 + \lambda_{12}|w_5|^2 + \lambda_{21}|w_7|^2) \rangle$$

$$D_b = 2r\langle (\lambda_{11}|w_2|^2 + \lambda_{12}|w_4|^2 + \lambda_{21}|w_6|^2) \rangle$$

$$D_z = r\langle \lambda_{01}|w_1|^2 \rangle$$

$$\begin{aligned} G_a = 2U\gamma\langle \mathrm{Im}\{ & (2F - \lambda_{11}) w_2 * w_3 \\ & + (2F - \lambda_{12}) w_4 * w_5 \\ & + 2(2F - \lambda_{21}) w_6 * w_7 \} \rangle \end{aligned}$$

$$\begin{aligned} G_b = 2U\gamma\langle \mathrm{Im}\{ & \lambda_{11} w_2 * w_3 + \lambda_{12} w_4 * w_5 \\ & + 2\lambda_{21} w_6 * w_7 \} \rangle \end{aligned}$$

$$\begin{aligned} C(Z,a) = \eta\langle X_1\, \mathrm{Im}\{ & (2F + \lambda_{01} - \lambda_{11}) w_2 * w_3 \\ & + \tfrac{1}{2}(2F + \lambda_{01} - \lambda_{12}) w_4 * w_5 \\ & + 2(2F + \lambda_{01} - \lambda_{21}) w_6 * w_7 \} \rangle \end{aligned}$$

$$\begin{aligned} C(A,a) = \varepsilon\langle \mathrm{Im}\{ & (2F - \lambda_{21}) X_3 * w_5 * w_6 \\ & - (2F - \lambda_{12}) X_3 * w_4 * w_7 \\ & + (2F - \lambda_{11}) w_2 * X_5 * w_7 \\ & - (2F - \lambda_{21}) w_3 * X_5 * w_6 \\ & + (2F - \lambda_{12}) w_3 * w_4 * X_7 \\ & - (2F - \lambda_{11}) w_2 * w_5 * X_7 \} \rangle \\ & + 2\Big\langle (2F + \lambda_{11})\, \mathrm{Im}(w_3 * X_3) \\ & \times \sum_{j=1}^{7} \mathrm{Re}(T_{1j} * w_j) \\ & + (2F + \lambda_{12})\, \mathrm{Im}(w_5 * X_5) \\ & \times \sum_{j=1}^{7} \mathrm{Re}(T_{2j} * w_j) \\ & + (2F + \lambda_{21})\, \mathrm{Im}(w_7 * X_7) \\ & \times \sum_{j=1}^{7} \mathrm{Re}(T_{3j} * w_j) \Big\rangle \end{aligned}$$

$$\begin{aligned} C(B,a) = \varepsilon\langle \mathrm{Im}\{ & (\lambda_{12} - \lambda_{21}) X_2 * w_5 * w_7 \\ & + (\lambda_{21} - \lambda_{11}) w_3 * X_4 * w_7 \\ & + (\lambda_{11} - \lambda_{12}) w_3 * w_5 * X_6 \} \rangle \end{aligned}$$

$$C(Z,b) = \eta\langle X_1\, \mathrm{Im}\{ (\lambda_{11} - \lambda_{01}) w_2 * w_3$$

$$+\tfrac{4}{5}(\lambda_{12}-\lambda_{01})w_4 * w_5$$
$$+2(\lambda_{21}-\lambda_{01})w_6 * w_7\}\rangle$$

$$C(A,b)=\varepsilon\langle \mathrm{Im}\{\lambda_{12}X_3 * w_5 * w_6$$
$$-\lambda_{21}X_3 * w_4 * w_7+\lambda_{21}w_2 * X_5 * w_7$$
$$-\lambda_{11}w_3 * X_5 * w_6+\lambda_{11}w_3 * w_4 * X_7$$
$$-\lambda_{12}w_2 * w_5 * X_7\}\rangle$$

$$C(B,b)=\varepsilon\langle \mathrm{Im}\{(\lambda_{12}-\lambda_{21})X_2 * w_4 * w_6$$
$$+(\lambda_{21}-\lambda_{11})w_2 * X_4 * X_6$$
$$+(\lambda_{11}-\lambda_{12})w_2 * w_4 * X_6\}\rangle$$
$$+2\lambda_{21}\Big\langle \mathrm{Im}(w_6 * X_6)$$
$$\times \sum_{j=1}^{7}\mathrm{Re}(T_{3j} * w_j)\Big\rangle$$

$$C(A,z)=-\eta\langle w_1\,\mathrm{Im}\{(2F+\lambda_{01}-\lambda_{11})w_2 * X_3$$
$$+\tfrac{4}{5}(2F+\lambda_{01}-\lambda_{12})w_4 * X_5$$
$$+2(2F+\lambda_{01}-\lambda_{21})w_6 * X_7\}\rangle$$

$$C(B,z)=-\eta\langle w_1\,\mathrm{Im}\{(\lambda_{11}-\lambda_{01})X_2 * w_3$$
$$+\tfrac{4}{5}(\lambda_{12}-\lambda_{01})X_4 * w_5$$
$$+2(\lambda_{21}-\lambda_{01})X_6 * w_7\}\rangle$$

$$C(z,a)=\eta\langle w_1\,\mathrm{Im}\{(2F+\lambda_{01}-\lambda_{11})X_2 * w_3$$
$$+\tfrac{4}{5}(2F+\lambda_{01}-\lambda_{12})X_4 * w_5$$
$$+2(2F+\lambda_{01}-\lambda_{21})X_6 * w_7\}\rangle$$

$$C(z,b)=\eta\langle w_1\,\mathrm{Im}\{\lambda_{11}-\lambda_{01})w_2 * X_3$$
$$+\tfrac{4}{5}(\lambda_{12}-\lambda_{01})w_4 * X_5$$
$$+2(\lambda_{21}-\lambda_{01})w_6 * X_7\}\rangle$$

$$C(a,b)=\varepsilon\langle \mathrm{Im}\{\lambda_{11}(X_3 * w_4 * w_7-X_3 * w_5 * w_6)$$
$$+\lambda_{12}(w_3 * X_5 * X_6-w_2 * X_5 * w_7)$$
$$+\lambda_{21}(w_2 * w_5 * X_7-w_3 * w_4 * X_7)\}\rangle \qquad (A.3)$$

where w_j^*, T_{jk}^* and X_j^* are complex conjugates of w_j, T_{jk} and X_j, respectively; and

$$\eta=16\gamma^{3/2}/(3\pi^2)$$

$$\varepsilon=3\gamma^{3/2}/\pi$$

$$T_{11}=\beta_{24}\,\mathrm{Re}(X_3)/X_2$$
$$T_{12}=(\beta_{21}-\Omega_3)/X_2$$
$$T_{13}=(\beta_{22}+\beta_{24}X_1)/X_2$$
$$T_{14}=\beta_{23}\,\mathrm{Re}(X_6)/X_2$$
$$T_{15}=\beta_{23}\,\mathrm{Re}(X_7)/X_2+i\beta_{23}\,\mathrm{Im}(X_7)/X_2$$
$$T_{16}=\beta_{23}X_4/X_2$$
$$T_{17}=\beta_{23}\,\mathrm{Re}(X_5)/X_2+i\beta_{23}\,\mathrm{Im}(X_5)/X_2$$
$$T_{21}=\beta_{44}\,\mathrm{Re}(X_5)/X_4$$
$$T_{22}=\beta_{43}\,\mathrm{Re}(X_6)/X_4$$
$$T_{23}=\beta_{43}\,\mathrm{Re}(X_7)/X_4+i\beta_{43}\,\mathrm{Im}(X_7)/X_4$$
$$T_{24}=(\beta_{41}-\Omega_5)/X_4$$
$$T_{25}=(\beta_{42}+\beta_{44}X_1)/X_4$$
$$T_{26}=\beta_{43}X_2/X_4$$
$$T_{27}=\beta_{43}\,\mathrm{Re}(X_3)/X_4+i\beta_{43}\,\mathrm{Im}(X_3)/X_4$$
$$T_{3j}=T_{1j}+T_{2j}\quad j=1,\ldots,7. \qquad (A.4)$$

Here, Ω_3 and Ω_5 are the 2 independent frequencies of the M-state, functionally related to the equilibrated state variables.

Except for the terms in the second angular bracket of $C(A,a)$ and $C(B,b)$, all the terms in (A.3) are the linearized counterparts of the energetic equations used in M85. Their physical interpretations are parallel to those in M85. The terms in the second angular bracket of $C(A,a)$ arise from the difference of the absolute angles of the baroclinic components of the perturbation from those of the M-state. Similarly, the terms in the second angular bracket of $C(B,b)$ arises from the difference of the absolute angles of the barotropic components of the perturbation from those of the M-state. Recall that the absolute angles of the barotropic components of the (1, 1) and (1, 2) waves may be absorbed into their baroclinic components. Hence, only the absolute angle of the barotropic component of the (2, 1) wave, which in effect measures the relative angle among all the barotropic components of the three waves, makes a contribution to this conversion rate.

REFERENCES

Charney, J. G. and DeVore, J. G. 1979. Multiple flow equilibria in the atmosphere and blocking. *J. Atmos. Sci. 36*, 1205–1216.

Chou, S.-H. and Loesch, A. Z. 1986. Supercritical dynamics of baroclinic disturbances in a free-surface model. *J. Atmos. Sci. 43*, 285–301.

Jones, S. 1979. Rossby wave interactions and instabilities in a rotating, two-layer fluid on a beta-plane. Part II: Stability. *Geophys. Astrophys. Fluid Dyn. 12*, 1–33.

Källén, E. 1981. The nonlinear effects of orographic and momentum forcing in a low-order, barotropic model. *J. Atmos. Sci. 38*, 2150–2163.

Klein, P. and Pedlosky, J. 1986. A numerical study of baroclinic instability at large supercriticality. *J. Atmos. Sci. 43*, 1263–1274.

Landford, O. E. 1981. Strange attractors and turbulence. In *Hydrodynamic instabilities and the transition to turbulence* (eds. H. L. Swinney and J. P. Gollub). *Topics in Applied Physics, Vol. 45*, Springer-Verlag, 7–26.

Legras, B. and Ghil, M. 1985. Persistent anomalies, blocking and variations in atmospheric predictability. *J. Atmos. Sci. 42*, 433–471.

Lorenz, E. N. 1963. The mechanics of vacillation. *J. Atmos. Sci. 20*, 448–464.

Lorenz, E. N. 1972. Barotropic instability of Rossby wave motion. *J. Atmos. Sci. 29*, 258–264.

Mak, M. 1985. Equilibration in nonlinear baroclinic instability. *J. Atmos. Sci. 42*, 2764–2782.

Pedlosky, J. 1970. Finite amplitude baroclinic waves. *J. Atmos. Sci. 27*, 15–30.

Pedlosky, J. 1981. Resonant topographic waves in barotropic and baroclinic flows. *J. Atmos. Sci. 38*, 2626–2641.

Powell, M. J. D. 1970. A hybrid method for nonlinear equations. In *Numerical methods for non-linear algebraic equations* (ed. P. Rabinowitz). Gordon and Breach, 87–114.

Rambaldi, S. and Mo, K. C. 1984. Forced stationary solutions in a barotropic channel: Multiple equilibria and theory of nonlinear resonance. *J. Atmos. Sci. 41*, 3135–3146.

Reinhold, B. 1986. Structural determinism of linear baroclinic waves and simple nonlinear equilibration. *J. Atmos. Sci. 43*, 1484–1504.

Smith, A. K. 1983. Observation of wave-wave interactions in the stratosphere. *J. Atmos. Sci. 40*, 2484–2496.

Smith, A. K., Gille, J. G. and Lyjak, L. V. 1984. Wave-wave interactions in the stratosphere: Observations during quiet and active wintertime periods. *J. Atmos. Sci. 41*, 363–373.

Tung, K. K. and Rosenthal, A. J. 1985. Theories of multiple equilibria—a critical reexamination. Part I. Barotropic models. *J. Atmos. Sci. 42*, 2804–2819.

Vautard, R. and Legras, B. 1986. Invariant manifolds, quasi-geostrophy and initialization. *J. Atmos. Sci. 43*, 565–584.

Vickroy, J. G. and Dutton, J. A. 1979. Bifurcation and catastrophe in a simple, forced, dissipative quasi-geostrophic flow. *J. Atmos. Sci. 36*, 42–52.

Wiin-Nielsen, A. 1979. Steady states and stability properties of a low-order barotropic system with forcing and dissipation. *Tellus 31*, 375–386.

Yoden, S. 1985. Bifurcation properties of a quasi-geostrophic barotropic low-order model with topography. *J. Meteorol. Soc. of Japan 63*, 535–546.